The Plant Journal (2007) doi: 10.1111/j.1365-313X.2007.03235.x

Carbon conversion efficiency and central metabolic fluxes in developing sunflower (*Helianthus annuus* L.) embryos

Ana P. Alonso[†,*], Fernando D. Goffman[‡], John B. Ohlrogge and Yair Shachar-Hill
Department of Plant Biology, Michigan State University, East Lansing, Michigan 48824, USA

Received 13 February 2007; revised 29 May 2007; accepted 14 June 2007.
[*]For correspondence (fax +33 561 559 689; e-mail ana-paula.alonso@insa-toulouse.fr).
[†]Present address: UMR5504, UMR792 Ingénierie des Systèmes Biologiques et des Procédés, CNRS, INRA, INSA, F-31400 Toulouse, France.[‡]Present address: Philip Morris International, R&D Department, Quai Jeanrenaud 56, 2000 Neuchatel, Switzerland.

Summary

The efficiency with which developing sunflower embryos convert substrates into seed storage reserves was determined by labeling embryos with [U-$^{14}C_6$]glucose or [U-$^{14}C_5$]glutamine and measuring their conversion to CO_2, oil, protein and other biomass compounds. The average carbon conversion efficiency was 50%, which contrasts with a value of over 80% previously observed in *Brassica napus* embryos (Goffman *et al.*, 2005), in which light and the RuBisCO bypass pathway allow more efficient conversion of hexose to oil. Labeling levels after incubating sunflower embryos with [U-$^{14}C_4$]malate indicated that some carbon from malate enters the plastidic compartment and contributes to oil synthesis. To test this and to map the underlying pattern of metabolic fluxes, separate experiments were carried out in which embryos were labeled to isotopic steady state using [1-$^{13}C_1$]glucose, [2-$^{13}C_1$]glucose, or [U-$^{13}C_5$]glutamine. The resultant labeling in sugars, starch, fatty acids and amino acids was analyzed by NMR and GC-MS. The fluxes through intermediary metabolism were then quantified by computer-aided modeling. The resulting flux map accounted well for the labeling data, was in good agreement with the observed carbon efficiency, and was further validated by testing for agreement with gas exchange measurements. The map shows that the influx of malate into oil is low and that flux through futile cycles (wasting ATP) is low, which contrasts with the high rates previously determined for growing root tips and heterotrophic cell cultures.

Keywords: fatty acid synthesis, sunflower embryo, metabolic flux analysis, carbon conversion efficiency, isotopic labeling, oilseed filling.

Introduction

The major metabolic function of developing seeds is to convert carbon and nitrogen precursors provided by the mother plant into stable reserves required for germination and seedling establishment. The efficiency of the overall metabolic processes involved in accumulating seed storage products will determine the amount of reserve material available for the next generation of a plant species. Plants would therefore be expected to have evolved pathways and mechanisms to maximize this efficiency. Many species (e.g. soybean, canola) have seeds that remain green while accumulating storage reserves. In previous studies of green *Brassica napus* embryos, we found that the conversion of carbohydrate to seed storage oil and protein is extremely efficient (Goffman *et al.*, 2005; Schwender *et al.*, 2004a). This efficiency can be attributed to light-driven provision of ATP and reductant, which allows the operation of the RuBisCO bypass – a novel metabolic route that allows more efficient conversion of hexose to oil – and also eliminates the need for a significant TCA cycle flux (Schwender *et al.*, 2006). To date, the efficiency of metabolism and the network of central metabolic fluxes have not been directly examined for non-green, heterotrophic seeds. Sunflower represents an example of such seeds as well as being a major oilseed crop, with an oil content of 55%.

Fatty acid synthesis in plants occurs predominantly in plastids and requires carbon in the form of acetyl CoA units as well as ATP and reducing power. Because acetyl CoA cannot cross the plastid membrane (Roughan *et al.*, 1979; Weaire and Kekwick, 1975), precursors for its synthesis must be generated in the plastid or imported from the cytosol.

Cytosolic metabolites such as glucose-6-phosphate (glucose-6-P), phospho*enol*pyruvate (PEP), pyruvate and malate have been shown to support fatty acid synthesis by isolated plastids (Eastmond and Rawsthorne, 2000; Kang and Rawsthorne, 1996; Kang *et al.*, 1994; Pleite *et al.*, 2005; Qi *et al.*, 1995; Smith *et al.*, 1992) . The capacity of plastids to convert these carbon sources into acetyl CoA differs between plant tissues and species. Fatty acid synthesis also requires reducing power in the form of NADH and NADPH. In green seeds, light energy can be used by chloroplasts to provide the ATP and NADPH necessary for fatty acid synthesis (Browse and Slack, 1985; Goffman *et al.*, 2005; Ruuska *et al.*, 2004; Schwender *et al.*, 2004a, 2006), whereas plastids isolated from heterotrophic tissues require added ATP for maximal rates of fatty acids synthesis (Browse and Slack, 1985; Hill and Smith, 1991; Kang and Rawsthorne, 1996; Kleppinger-Sparace *et al.*, 1992; Neuhaus *et al.*, 1993; Smith *et al.*, 1992).

Rawsthorne (2002) gives an overview of the carbon and reductant sources for fatty acid synthesis. The ATP and reducing power necessary for fatty acid synthesis in non-photosynthetic tissues such as developing sunflower embryos can in principle be produced during the synthesis of acetyl CoA from glucose-6-P, malate, PEP or pyruvate or via the plastidic oxidative pentose phosphate pathway (OPPP). Pleite *et al.* (2005) showed that, when different carbon sources were supplied to plastids isolated from developing sunflower embryos, malate supported the highest rates of fatty acid synthesis throughout the period of oil accumulation. It was proposed that reducing power could be generated via plastidic malic enzyme (EC 1.1.1.40) and pyruvate dehydrogenase. However, pyruvate supported substantial rates of fatty acid synthesis when incubations also included glucose-6-P. Although these *in vitro* studies reveal a range of possible routes for metabolism, the proportions of fatty acids that developing embryos actually synthesize from malate or hexose phosphates and the respective proportions of reductant generated from malate or via the OPPP *in vivo* remain undetermined.

To better understand fatty acid synthesis in developing sunflower seeds, we studied carbon metabolism in the whole embryo, which can provide information not only on the nature of the sources of carbon and reductant but also on the fluxes of primary metabolism. There are several approaches to quantify multiple metabolic fluxes in plant systems (Ratcliffe and Shachar-Hill, 2006). One consists of measuring final product accumulation or substrate disappearance with time (flux balance analysis). The rates thus obtained are net fluxes, i.e. the difference between synthesis and degradation rates, are dependent on a known or assumed metabolic network, and contain little information on subcellular compartmentation. Other approaches involve either pulsed or steady-state isotopic labeling using radioactive or stable tracers. Pulsed labeling experiments with radioactive tracers allow measurement of unidirectional fluxes of synthesis such as sucrose synthesis from the rate of the incorporation of radioactivity into sucrose (e.g. Alonso *et al.*, 2005; Hargreaves and ap Rees, 1988; Hatzfeld and Stitt, 1990; Hill and ap Rees, 1994, 1995) . On the other hand, in steady-state labeling experiments using stable isotopes (Dieuaide-Noubhani *et al.*, 1995; Rontein *et al.*, 2002; Schwender *et al.*, 2003, 2004a, 2006; Sriram *et al.*, 2004), fluxes are calculated from equations describing the input and output fluxes of label at the level of each atomic position of metabolites. Steady-state isotopic labeling flux analysis using ^{13}C-labeling, NMR and GC-MS analysis of labeled metabolites with computer-aided modeling is the only way available so far to simultaneously determine multiple fluxes through the network of central metabolism in plants (Ratcliffe and Shachar-Hill, 2005, 2006; Schwender *et al.*, 2004b).

Analyses of carbon metabolism in heterotrophic tissues such as tomato cells in culture and maize root tips revealed high fluxes through the oxidative pentose-P pathway and the tricarboxylic acid (TCA) cycle. Substantial proportions of the ATP produced in those tissues were also found to be consumed by futile cycling (Alonso *et al.*, 2005; Dieuaide-Noubhani *et al.*, 1995; Rontein *et al.*, 2002). These results are intriguing as there is no obvious purpose served by this high degree of futile cycling, and one would expect that selection pressures during evolution would favour a higher degree of efficiency of carbon use. This pressure would seem to be especially acute in the formation of seed storage compounds, on whose efficient production the reproductive competitiveness of a plant is critically dependent.

In the present study, we have quantified the fluxes through the primary metabolic network in developing sunflower embryos during oil accumulation, and addressed questions about carbon conversion efficiency and the extent of futile cycling as well as the routes of carbon flow into oil and the origins of the reducing power necessary for fatty acid synthesis.

Results

Sunflower embryo culture

According to confocal microscopic observations, sunflower embryos are closely associated with maternal vascular tissue (Ben *et al.*, 2005). In order to identify the metabolites available to the embryo and measure their levels, ethanolic extracts from vascular tissues collected 12 days after pollination (DAP) were analyzed by ^{1}H-NMR (Figure S1). Sucrose, glucose, alanine, glutamine and fumaric acid were identified in the extracts at 13 ± 2, 94 ± 15, 1.0 ± 0.5, 6 ± 1 and 5.0 ± 0.1 mM, respectively. This composition was found to be very similar to that in phloem (data not shown). Thus glucose and glutamine account for >80% of the sugar and amino acid pools. Accordingly, glucose and glutamine were

provided as the major carbon and nitrogen sources for culture of sunflower embryos. In cultures where the concentrations of glucose and glutamine were 400 and 70 mM, respectively, the embryo dry weight accumulation (1.35 ± 0.36 mg embryo^{-1} day^{-1}) was indistinguishable from *in planta* growth rates (1.47 ± 0.22 mg embryo^{-1} day^{-1}). The composition of storage biomass by embryos developing under these conditions was also similar to that of embryos developing *in planta*, with the cultured embryos having somewhat more starch and less oil than the embryos growing *in planta*; cell wall and protein contents were not significantly different (Figure 1).

Carbon conversion efficiency

Carbon mass balancing is used in order to estimate the efficiency with which metabolites are transformed into storage biomass products in micro-organisms (Converti and Perego, 2002; Novak and Loubiere, 2000; Saez *et al.*, 2002) as well as in plants (Flinn *et al.*, 1977; Goffman *et al.*, 2005; Pate *et al.*, 1977; Peoples *et al.*, 1985; Schwender *et al.*, 2004a). Glucose and/or glutamine or malate uniformly labeled with ^{14}C were supplied to developing sunflower embryos, and their metabolic fates were determined by measuring ^{14}C incorporation into biomass pools (starch, oil, proteins and cell walls) and released as $^{14}CO_2$ (Figure 2). Figure 2a shows the partitioning of the ^{14}C carbon after labeling with [U-$^{14}C_6$]glucose and [U-$^{14}C_5$]glutamine for 5 days (from 12 to 17 DAP): $20.0 \pm 3.8\%$, $11.1 \pm 0.8\%$, $5.3 \pm 1.2\%$ and $13.1 \pm 0.8\%$ of the ^{14}C was incorporated into oil, protein, starch and cell walls, respectively, which represents a carbon conversion efficiency of 49.5%. Carbon partitioning after labeling with [U-$^{14}C_4$]malate (Figure 2b) or [U-$^{14}C_5$]glutamine (Figure 2c) showed a very similar pattern for ^{14}C incorporation in to CO_2, cell wall and starch. Label from [U-$^{14}C_5$]glutamine (Figure 2c) is incorporated much more into proteins than oil, while that from [U-$^{14}C_4$]malate is integrated equally into proteins and oil (Figure 2b). These results suggest that malate could be a precursor for fatty

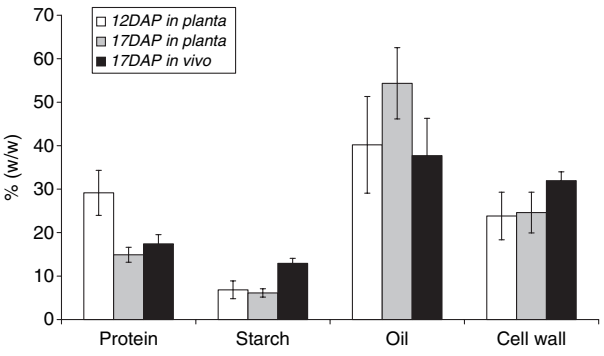

Figure 1. Biomass composition in developing sunflower embryos.
Biomass composition was determined for sunflower embryos harvested from the plant at 12 days after pollination (DAP), 17 DAP and embryos cultured from 12 to 17 DAP. Errors bars represent standard deviations of three independent experiments for 12 DAP embryos and four independent experiments for 17 DAP embryos *in planta* and *in vivo*.

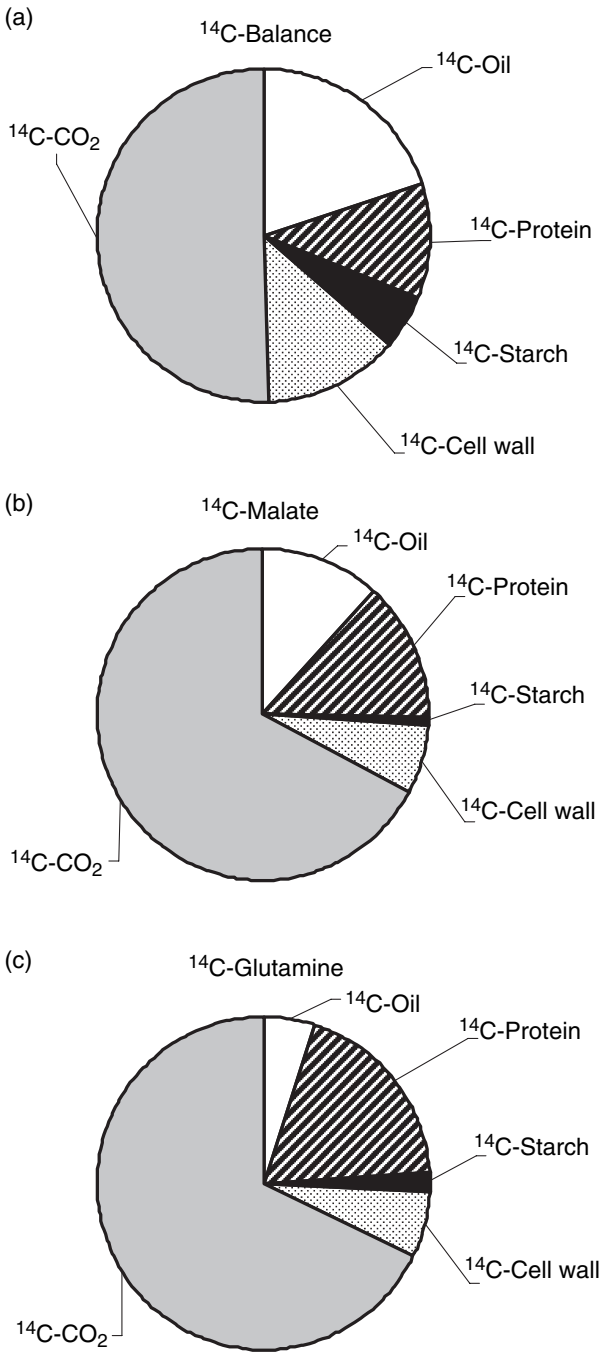

Figure 2. Distribution of ^{14}C-labeling among biomass fractions and CO_2.
(a) [U-$^{14}C_6$]glucose + [U-$^{14}C_5$]glutamine, (b) [U-$^{14}C_4$]malate + unlabeled glucose and glutamine, and (c) [U-$^{14}C_5$]glutamine + unlabeled glucose. Embryos were cultured at 27°C for 5 days in the presence of U-^{14}C carbon supplies. After culture, the $^{14}CO_2$ was collected by flushing the flasks through a trapping system, and the embryos were frozen in liquid N_2 for analysis of ^{14}C-labeling in biomass components. The proportions shown represent the ^{14}C recovered in the respective fractions.

acid synthesis *in vivo*. However, malate is not apparently provided to sunflower embryos *in planta* (Figure S1), and, furthermore, the above radiolabeling experiments cannot elucidate whether malate taken up by the embryo enters the plastid intact or is metabolized first. Accordingly, we used ^{13}C- and ^{14}C-labeling to elucidate the routes and rates of carbon flux.

Metabolic fluxes in developing sunflower embryos

Carbon-uptake and biomass accumulation. Glutamine and glucose-uptake rates were estimated to be 69 ± 11 and 558 ± 39 nmol h^{-1} $embryo^{-1}$, respectively, based on ^{14}C levels in embryos supplied with [U-$^{14}C_5$]glutamine + [U-$^{14}C_6$]glucose and [U-$^{14}C_5$]glutamine + unlabeled glucose. Oil bodies and protein levels in sunflower embryos increase linearly with time from 10–12 to 25–30 DAP (Mantese *et al.*, 2006; Ploschuk and Hall, 1997), suggesting that metabolism in developing sunflower embryos is at steady state between 12 and 25 DAP. The rates of biomass synthesis and metabolite accumulation were calculated by measuring the biomass accumulated during 5 days of culture (between 12 and 17 DAP). The rates of protein, starch, oil and cell-wall synthesis were 26.6 ± 4.7, 19.5 ± 1.9, 260.1 ± 74.0, 46.1 ± 3.4 nmol h^{-1} $embryo^{-1}$, respectively. Sucrose and glucose accumulation were found to be 24 ± 3 and 24 ± 7 nmol h^{-1} $embryo^{-1}$, respectively.

^{13}C-labeling. For metabolic flux analysis based on isotopic labeling to be valid, isotopic steady state must have been reached. This was confirmed by incubating sunflower embryos transferred into culture at 12 DAP with 50% [1-$^{13}C_1$]glucose for 5 and 7 days. Labeling in carbohydrates (sucrose, glucose and starch) and in free amino acids (alanine and glutamine) was analyzed using ^{1}H-NMR and ^{13}C-NMR to measure the enrichment of ^{13}C in each carbon position. The enrichments for these compounds after 7 days were all within 6% of the values at 5 days of labeling (data not shown), which confirmed that isotopic steady state is reached within 5 days of labeling.

The results described below are based on three separate experiments, in which developing embryos were labeled with 50% [1-$^{13}C_1$]glucose (n = 3 biological replicates), 100% [2-$^{13}C_1$]glucose (n = 2) or 100% [U-$^{13}C_5$]glutamine (n = 1) for 5 days. After extraction, oil, starch and hydrolysable molecules (free sugars and amino acids) were analyzed by ^{1}H-NMR and ^{13}C-NMR (Figure 3). Protein extracts were hydrolyzed, derivatized and analyzed by GC-MS (Figure 4). The full NMR and GC-MS datasets are reported in Tables S2 and S3, respectively.

Building a model of sunflower embryo central metabolism. The metabolic network was defined from information available in the literature on sunflower embryos (Hewezi *et al.*, 2006; Pleite *et al.*, 2005) and other heterotrophic plant tissues (Dieuaide-Noubhani *et al.*, 1995; Rontein *et al.*, 2002) and from the labeling data. We used existing models of metabolic pathways in non-photosynthetic tissues to which oil and protein synthesis pathways were added (Schwender *et al.*, 2006). Incorporation of [U-$^{14}C_4$]malate and [U-$^{14}C_5$]glutamine into starch and cell wall (Figure 2b,c) indicated a gluconeogenic flux that was also included as reversibility of the glycolytic flux and phosphoenolpyruvate carboxylase (PEPC). [U-$^{14}C_4$]malate labeling suggested that malate can be a precursor for oil synthesis in sunflower embryos (Figure 2b), which was considered in our model by adding a NADP-dependent malic enzyme (EC 1.1.1.40) in the plastid. As previously shown in maize root tips (Dieuaide-Noubhani *et al.*, 1995), the observation of a substantial loss of label in the C1 carbon position of starch glucosyl units after labeling with [1-$^{13}C_1$]glucose (Table S2), and the low transfer of label from C2 to C1 observed in sucrose and glucose compared to starch after labeling with [2-$^{13}C_1$]glucose (Table S2), suggest that the OPPP is mainly located in the plastid of sunflower embryos. Detailed equations describing the network of central carbon metabolism in developing sunflower embryos are presented in Table S1.

The 13C-FLUX® software package was used for quantifying flux values (Mollney *et al.*, 1999; Wiechert and de Graaf, 1997; Wiechert *et al.*, 1997, 1999). The following data were used in modeling: (i) the ^{13}C-labeling data obtained with the three different labeling experiments (50% [1-$^{13}C_1$]glucose, 100% [2-$^{13}C_1$]glucose and 100% [U-$^{13}C_5$]glutamine; Tables S2 and S3), (ii) the equations describing carbon metabolism (Table S1), (iii) the rates of glucose and glutamine uptake determined in ^{14}C-labeling experiments, and (iv) the rates of accumulation of each biomass component determined during the 5 days of culture. In order to include data from the three separate experiments ([1-$^{13}C_1$]glucose, [2-$^{13}C_1$]glucose and [U-$^{13}C_5$]glutamine) into a single flux estimation procedure, each flux and metabolite pool was encoded three times. 13C-FLUX® evaluates a set of stoichiometrically feasible fluxes that best accounts for the measured data. The flux optimization was repeated (Monte Carlo optimization) over 2000 times from different starting points, and over 69% of the optimization runs converged to a very similar set of flux values that yielded the best fit to the experimental data. Confidence intervals for each flux were determined from the range of measured labeling values obtained in different experiments (biological variation) and the sensitivity of each flux value to variation in the different measurements. The resulting flux map and the values for forward and reverse fluxes are shown in Figure 5 and Table 1 together with their confidence intervals.

Model validation. One way to test the validity of our modeling analysis is to compare the rate of CO_2

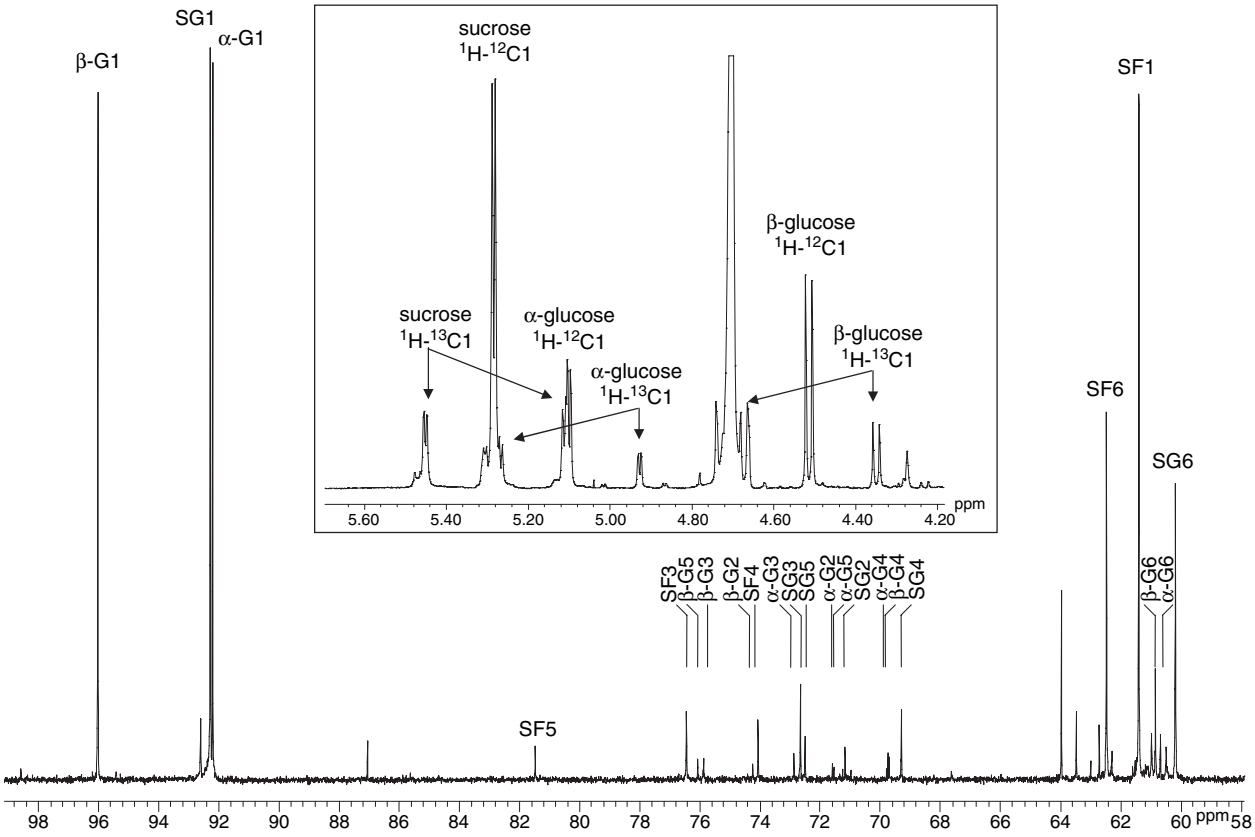

Figure 3. ^{13}C and ^{1}H spectra (inset) of cellular sugars.
Sunflower embryos were incubated for 5 days with 50% [1-$^{13}C_1$]glucose. The sugar fraction was purified and analyzed by ^{1}H and ^{13}C-NMR as described in Experimental procedures. α-G*n*, β-G*n*, SG*n* and SF*n* correspond to the resonance of carbon *n* of α and β glucose, and of the glucosyl and fructosyl moieties of sucrose, respectively. For the studied carbon atoms, the enrichment values were obtained as described by Alonso *et al.* (2005).

production predicted by the model to that determined experimentally, as this measured flux value was not included in the modeling process. The model calculates a CO_2 production rate of 2064 ± 53 nmol CO_2 h^{-1} $embryo^{-1}$, which is close to the CO_2 production directly measured by gas analysis (1705 ± 221 nmol CO_2 h^{-1} $embryo^{-1}$). The validity of the modeling results was further tested by comparing the rate of O_2 consumption predicted by the model to that we measured for cultured developing sunflower embryos. The flux through reactions producing NADH in the cytosol and mitochondria (pyruvate dehydrogenase, isocitrate dehydrogenase, malate dehydrogenase, α-ketoglutarate dehydrogenase, succinate dehydrogenase, fumarase, malic enzyme and glyceraldehyde-3-P dehydrogenase) was estimated by the flux modeling to produce between 3073 and 3747 nmol of NADH h^{-1} $embryo^{-1}$ depending on the localization of the glyceraldehyde-3-P dehydrogenase. As 2 mol of NADH are required to reduce 1 mol of O_2, the rate of oxygen consumption estimated by the model is between 1537 and 1874 nmol O_2 h^{-1} $embryo^{-1}$. These values are very close to the rate of O_2 consumption determined experimentally (1854 ± 231 nmol O_2 h^{-1} $embryo^{-1}$), which furnishes additional independent validation of the model. The close agreement between calculated versus measured labeling data shown in Figure 6 indicates that the mathematical flux model adequately describes the experimentally observed data.

Metabolism in sunflower embryos

Precursors and reducing power for fatty acid synthesis Major questions about oilseed metabolism concern the route of carbon flow from maternally supplied substrates into seed oil and how reductant is generated for fatty acid synthesis. Based on analysis of the labeling results (Figure 5 and Table 1), 91–95% of the carbon for fatty acid synthesis is derived from triose phosphate produced from hexose that is imported into the plastid. Only 5–9% of the carbon for fatty acid synthesis was attributable to the import of malate. Similarly, substantial uptake of pyruvate into the plastid was not supported by our labeling data, as clearly indicated from significantly different labeling of alanine and acetyl CoA units (Table S2).

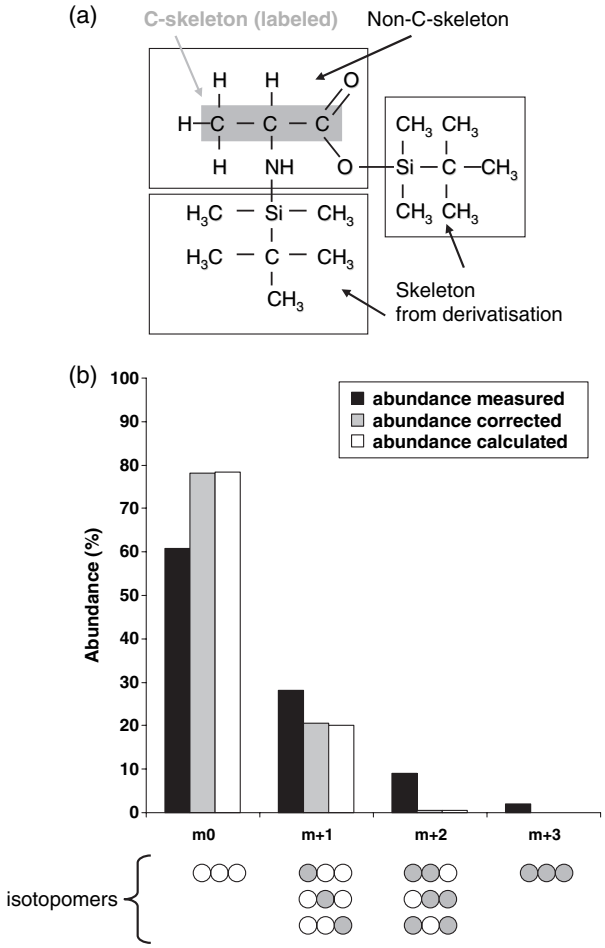

Figure 4. Determination by GC-MS of the isotopomer abundance in amino acids from protein hydrolysis, using alanine as an example.
After acid hydrolysis of the ^{13}C-proteins, amino acids obtained were derivatized with TBDMS and analyzed in GC-MS. For example, ^{13}C-alanine derivatization produced the compound shown in (a) with attachment of the derivative to the carboxyl and amine groups.
(b) The mass spectrum of this compound (black bars). A correction is made in order to quantify the isotopomers of ^{13}C-alanine : the masses and natural abundances of the isotopes of C, N, Si, H, O that are not part of the carbon skeleton of alanine have to be accounted for. The result of this correction is presented in gray, and is directly comparable to the abundances calculated by the model (white bars). Peaks m0, m + 1, m + 2 and m + 3 are alanine isotopomers containing respectively 0, 1, 2 and 3 atoms of ^{13}C.

Thus most carbon from the cytosol enters the plastid at the level of hexoses, and malate appears not to be a major source of carbon or of reductant for plastidic fatty synthesis during sunflower embryo development. Net forward flux through the upper part of glycolysis appears to be confined to the plastid, but the subcellular location of the lower part of glycolysis cannot be determined from our data. Carbon for the net gluconeogenic flux in the cytosol is supplied largely by triose phosphate export from the plastid. Because the subcellular location of reactions between triose phosphate and PEP cannot be distinguished by these experiments, we cannot rule out the possibility that some PEP is imported into plastids after its formation in the cytosol.

The oxidative pentose phosphate pathway (OPPP), localized in the plastid, provides enough reductant for oil production. The calculated OPPP flux can produce 550 $\pm$ 36 nmol NADPH h^{-1} $embryo^{-1}$, whereas the measured rate of fatty acid synthesis requires 259 $\pm$ 16 nmol NADPH h^{-1} $embryo^{-1}$. Thus the calculated OPPP flux generates sufficient NADPH for fatty acid production without the need for flux through plastidic NADP-dependent malic enzyme. Alternative modeling of our labeling data using models with a partial or complete cytosolic OPPP suggests that there is no significant cytosolic OPPP activity. This is further strongly suggested by the different labeling of sucrose and starch glucosyl units (Table S2). Thus plastidic OPPP flux can provide all the NADPH needed for fatty acid synthesis, and plastidic pyruvate dehydrogenase is estimated to provide all the NADH necessary (260 $\pm$ 16 nmol NADH h^{-1} $embryo^{-1}$).

Low fluxes through substrate cycles. Previous studies of heterotrophic plant tissues (maize root tips and tomato cell suspensions) have indicated a high rate of ATP consumption through substrate cycles (Dieuaide-Noubhani *et al.*, 1995; Rontein *et al.*, 2002). The rate of O_2 consumption by sunflower embryos was measured experimentally and found to be 1854 $\pm$ 231 nmol h^{-1} $embryo^{-1}$. According to Zaitseva *et al.* (2002), the ADP/O (ATP produced over oxygen consumed) ratio is close to one in mitochondria of 13 DAP sunflower embryos, which means that a total of 3708 nmol ATP h^{-1} $embryo^{-1}$ could be produced via mitochondrial respiration. According to our flux model (Figure 5), 1348 nmol ATP h^{-1} $embryo^{-1}$ should be formed by glycolysis, leading to a total ATP production of 5056 nmol ATP h^{-1} $embryo^{-1}$. In developing sunflower embryos, triose-P/hexose-P cycling occurs between the cytosol and the plastid compartments (Figure 5), and consumes a maximum of 320 nmol ATP h^{-1} $embryo^{-1}$, depending on the enzyme(s) involved in the conversion of fructose-1,6-bisP to fructose-6-P. The equivalent of one ATP is consumed if this reaction is catalyzed by fructose-1,6-bisphosphatase, but none if it catalyzes by the PPi-dependent phosphofructokinase. Thus, the maximum consumption of ATP by the triose-P/hexose-P cycle is 6% of the ATP produced by respiration. For the cycling between hexose-P and glucose, the synthesis and breakdown of sucrose and/or glucose-6-P phosphatase activity may be involved (Alonso *et al.*, 2005). In the case of glucose-6-P phosphatase activity, a single ATP equivalent is used by the cycling, whereas sucrose synthesis by sucrose-P synthase and degradation by invertase requires two ATP if we consider that PPi is a donor of phosphate like ATP (Hill and ap Rees, 1994). Thus, hexose-P↔glucose cycling consumes between 344 and 688 nmol ATP h^{-1} $embryo^{-1}$, which

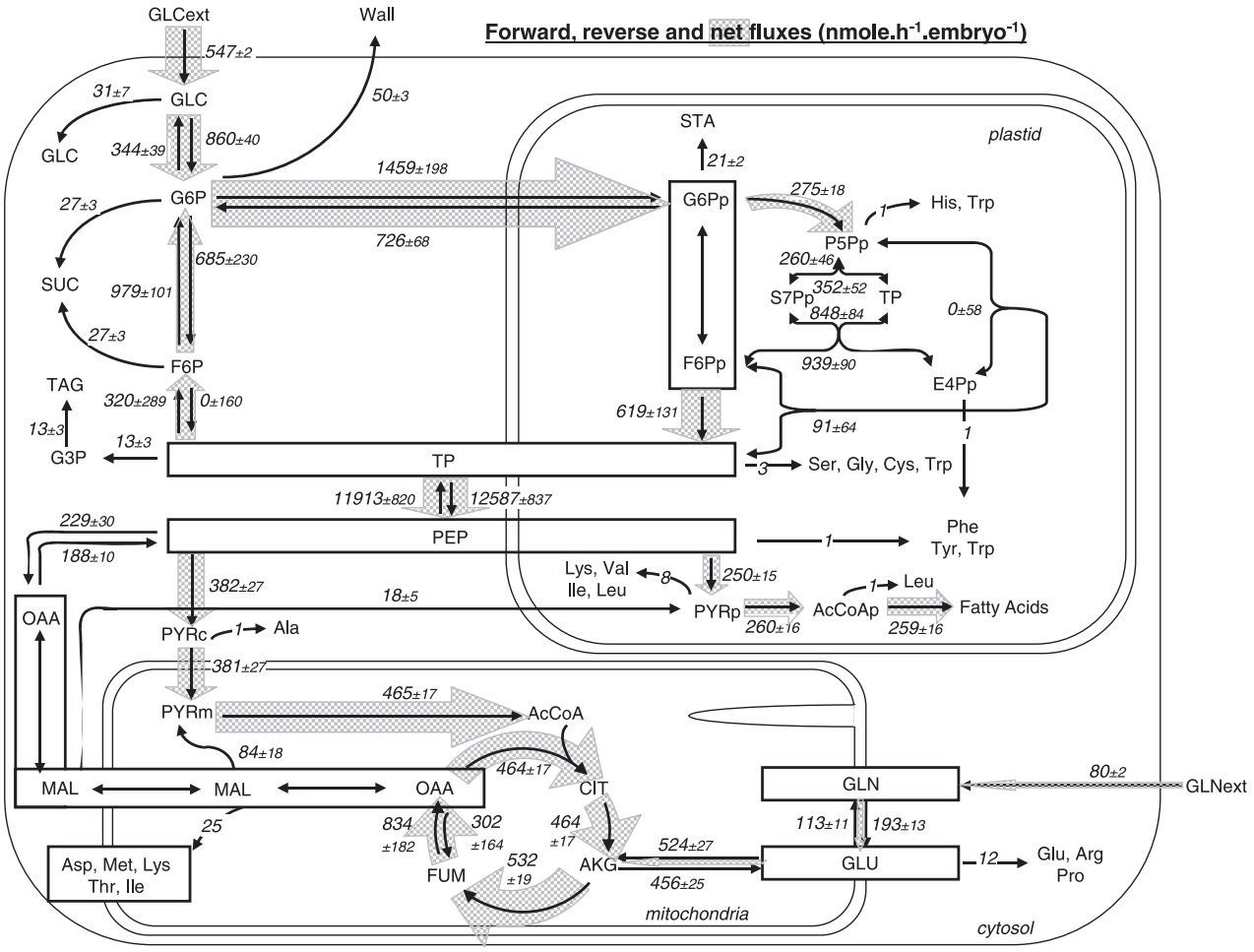

Figure 5. Metabolic network and fluxes in developing sunflower embryos.
The scheme shown is a simplified overview indicating steps for which our model allows calculations of fluxes and their localization. Values reported are the best fit and the ones most commonly obtained by optimized fitting, and are given as flux values (nmol molecule h^{-1} $embryo^{-1}$ ± confidence interval). For the net fluxes, the widths of the gray arrows are directly proportional to flux values. The boxes surrounding metabolites indicate that any differences in the labeling between these metabolites cannot be distinguished by our experiments. For example, labeling data do not allow the cytosolic and plastidic triose phosphate and PEP pools to be distinguished, and therefore the subcellular localization of these metabolites and their inter-conversion are indicated as undefined.

represents 7–14% of the ATP produced. Therefore, developing sunflower embryos utilize a maximum of 20% of the ATP produced in substrate cycles, which is in agreement with the high carbon conversion efficiency that we measured and much lower than levels of 45–70% that have been reported for other plant heterotrophic tissues (Alonso *et al.*, 2005; Dieuaide-Noubhani *et al.*, 1995; Rontein *et al.*, 2002).

ATP requirement for biomass synthesis in developing sunflower embryos. Fatty acid, starch and cell-wall synthesis require 1 mol ATP per mol acetyl CoA, ADP-glucose and UDP-glucose, respectively, whereas 4.3 mol ATP per amino acid attached are necessary for protein synthesis (Schwender *et al.*, 2006). Thus, fatty acid, starch, protein and cell-wall synthesis consume 259, 21, 224 and 50 nmol ATP h^{-1} $embryo^{-1}$, respectively. Consequently, only about 11% of the ATP produced is used for biomass production. Additional ATP is presumably consumed to power the import of the carbohydrate and amino acid precursors of storage end products and for cellular maintenance.

Discussion

A primary aim of this study was to quantify the fluxes through the central metabolic network in developing sunflower embryos in order to answer questions about carbon conversion efficiency, the routes of carbon flow into oil, and the origins of the reducing power necessary for fatty acid synthesis. Although there was some difference in biomass composition between sunflower embryos growing in culture and *in planta* (Figure 1), as has been

Table 1 Metabolic fluxes in developing sunflower embryos. Fluxes are given in nmol molecule h^{-1} $embryo^{-1}$

		Flux values (nmol molecule h^{-1} $embryo^{-1}$)	
Flux name	Flux or rate description	Forward	Backward
Vg	Rate of glucose uptake	547 ± 2	0
Va	Rate of glutamine uptake	80 ± 2	0
Vhk	Flux through hexokinase	860 ± 40	0
Vres	Fluxes from G6P to glucose	344 ± 39	0
Vgf	Fluxes catalyzed by G6P isomerase	685 ± 230	979 ± 101
Vald	Fluxes catalyzed by cytosolic aldolase	0 ± 160	320 ± 289
Vglyco	Glycolytic flux	12 587 ± 837	11 913 ± 820
Vfas2	Rate of glycerol incorporation into triacylglycerol	13 ± 3	0
Vsuc1	Flux of G6P to sucrose accumulation	27 ± 3	0
Vsuc2	Flux of F6P to sucrose accumulation	27 ± 3	0
Vglc	Rate of glucose accumulation	31 ± 7	0
Vgl	Flux of glutamine to glutamate	193 ± 13	113 ± 11
Vakg	Flux of glutamate to α-ketoglutarate	524 ± 27	456 ± 25
Vhcp	Exchange of cytosolic and plastidic hexose-P	1459 ± 198	726 ± 68
Valdp	Fluxes catalyzed by plastidic aldolase	619 ± 131	0
Vppp1	Flux of the oxidative part of the pentose-P pathway	275 ± 18	0
Vppp2	Fluxes catalyzed by transketolase	352 ± 52	260 ± 46
Vppp3	Fluxes catalyzed by transaldolase	939 ± 90	848 ± 84
Vppp4	Fluxes catalyzed by transketolase	91 ± 64	0 ± 58
Vpkp	Flux catalyzed by plastidic pyruvate kinase	250 ± 15	0
Vpdhp	Flux catalyzed by plastidic pyruvate dehydrogenase	260 ± 16	0
Vmep	Flux catalyzed by plastidic malic enzyme	18 ± 5	0
Vfas2	Flux of AcCoA to fatty acid synthesis	259 ± 15	0
Vpk	Flux catalyzed by pyruvate kinase	382 ± 27	0
Vpyr	Flux of pyruvate from cytosol to mitochondria	381 ± 27	0
Vpepc	Anaplerotic flux through PEPC	229 ± 30	188 ± 10
Vpdh	Flux catalyzed by pyruvate dehydrogenase	464 ± 17	0
Vcs	Flux through citrate synthase	464 ± 17	0
Vca	Flux calatyzed by aconitase	464 ± 17	0
Vsfa	Flux through 2-oxoglutarate dehydrogenase	532 ± 19	0
Vfum	Flux catalyzed by fumarase	834 ± 182	302 ± 164
Vme	Flux through malic enzyme	84 ± 18	0
Vco_2	Rate of CO_2 production	2064 ± 53	0
Vwall	Rate of cell-wall synthesis	50 ± 3	0
Vsta	Rate of starch accumulation	21 ± 2	0
Vp5peff	Flux of P5Pp to amino acids for protein synthesis	1	0
Vtpeff	Flux of TP to amino acids for protein synthesis	3	0
Vpepeff	Flux of PEP to amino acids for protein synthesis	1	0
Ve4peff	Flux of E4Pp to amino acids for protein synthesis	1	0
Vpyrpeff	Flux of PYRp to amino acids for protein synthesis	8	0
VAcCoAeff	Flux of AcCoAp to amino acids for protein synthesis	1	0
Vpyrceff	Flux of PYR to amino acids for protein synthesis	1	0
Voaaeff	Flux of OAA to amino acids for protein synthesis	25	0
Vglueff	Flux of GLU to amino acids for protein synthesis	12	0

Some fluxes were determined by ^{14}C-labeling experiments, such as the rate of glucose uptake (Vg) and the rate of glutamine uptake (Va). The rates of starch (Vsta), cell-wall (Vwall), protein, fatty acids (Vfas1 and Vfas2), sucrose (Vsuc1 and Vsuc2) and glucose (Vglc) accumulation were quantified by measuring their accumulation during the incubation period. Those results are reported as means ± SD. The flux of glucose resynthesis from hexose-P (Vres) was calculated using the equation: ($Vres = Vg \cdot (G_{ex}1/Sg6 - G_{in}1/G_{in}6 \cdot G_{ex}6/Sg6)/(G_{in}1/G_{in}6 - Sg1/Sg6)$, where $G_{ex}1$, Sg1 and $G_{in}1$ represent the enrichment of carbon 1 of extracellular glucose, the glucosyl moiety of sucrose and intracellular glucose, respectively, and $G_{ex}6$, Sg6 and $G_{in}6$ represent the enrichments of carbon 6 in the same molecules) [Equation (4) in Alonso *et al.* (2005)], and then entered as a free flux in the model. The other flux values were calculated from the model based upon carbon enrichment measured after steady-state labeling with [1-$^{13}C_1$]glucose, [2-$^{13}C_1$]glucose or [U-$^{13}C_5$]glutamine. The values are the best fit, and are also the most frequently determined optimized flux values ± confidence interval.

previously observed for culture of oilseeds (Hsu and Obendorf, 1982; Sriram *et al.*, 2004), the rate of dry weight accumulation is not significantly different. Overall, this study provided estimates of more than 50 central metabolic fluxes (Figure 5) through central metabolism in a developing non-green seed.

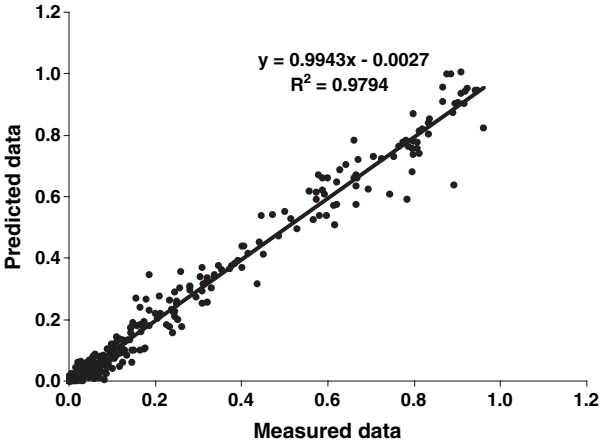

Figure 6. Comparison between predicted and measured data.
Scatter plot between the data calculated by the model and the measurements. The linear regression, equation and R^2-value are shown.

Carbon conversion efficiency in developing sunflower embryos

Sunflower embryos converted carbon supplies into reserves with an average efficiency of 50%, which is high compared to previously studied heterotrophic plant tissues (Dieuaide-Noubhani *et al.*, 1995; Rontein *et al.*, 2002), but contrasts with an efficiency of over 80% observed for the green embryos of *B. napus* (Goffman *et al.*, 2005). According to the data published by Sriram *et al.* (2004), the carbon conversion efficiency in soybean embryos growing at 100 μE m^{-2} sec^{-1} can be estimated at 55% (ratio between C assimilated into biomass and C input), which is very close to that measured in sunflower embryos. According to the flux map (Figure 5), 70% of the total CO_2 released by developing sunflower embryos was produced by the TCA cycle, compared to 13% each by OPPP and plastid pyruvate dehydrogenase. In *B. napus* embryos, there was no net flux round the TCA cycle, and therefore mitochondrial reactions provided much less reductant or energy for biomass accumulation (Schwender *et al.*, 2006). Instead, in these green seeds, the light reactions of photosynthesis can provide both ATP and reductant, and the RuBisCO bypass allows more efficient conversion of hexose to oil (Goffman *et al.*, 2005; Schwender *et al.*, 2004a). In contrast, in soybean embryos, the oxidative part of the pentose-P pathway and pyruvate dehydrogenase produce 40% and 34% of the total CO_2 released, respectively, also furnishing a large amount of the reductant (NADPH and NADH) required for fatty acid synthesis (Sriram *et al.*, 2004). In soybean embryos, flux through the TCA cycle is very low, and ATP is presumably provided by photosynthesis and high flux through glycolysis. In the case of sunflower embryos, the high flux through the TCA cycle coupled to NADH oxidation produced ATP at a high rate. The amount of ATP consumed by futile cycling represented <20% of the total ATP produced, which is in agreement with the carbon efficiency measured, and contrasts with other heterotrophic tissues such as maize root tips where around 45% of the ATP was dissipated by substrate cycling (Alonso *et al.*, 2005). Because of the loss of CO_2 in the pyruvate dehydrogenase reaction, fatty acid synthesis coupled to glycolysis results in a maximum theoretical carbon efficiency of 66%, whereas carbohydrate and protein storage can result in carbon efficiencies of > 95% and 80%, respectively. Our data indicate that sunflower embryos, which mainly accumulate fatty acids, have a carbon efficiency of 50%. In comparison, other heterotrophic tissues such as maize root tips and tomato cells in culture, which produce mainly carbohydrate, have efficiencies of 47% and 58%, respectively (A.P. Alonso, P. Raymond, M. Hernould, C. Rondeau-Mouro, A. de Graaf, P. Chourey, M. Lahaye, Y. Shachar-Hill, D. Rolin and M. Dieuaide-Noubhani, unpublished results; Rontein *et al.*, 2002). Thus sunflower embryos have a high carbon efficiency considering they are a heterotrophic tissue in which fatty acids are the major end product of metabolism. This efficiency probably evolved under selection pressure to provide maximum carbon storage to support germination and seedling development.

Carbon and reductant sources for oil synthesis in developing sunflower embryos

In *B. napus* embryos, carbon for fatty acid synthesis was provided by 3-phosphoglycerate derived from the RuBisCo reaction and glycolysis, and NAPDH and ATP could be largely supplied by light (Goffman *et al.*, 2005; Ruuska *et al.*, 2004; Schwender *et al.*, 2004a, 2006). In soybean embryos, 95% of plastidic acetyl CoA is apparently made from triose-P and only 5% by malate; NADPH and NADH could be supplied by the oxidative part of the pentose-P pathway and by pyruvate dehydrogenase (Sriram *et al.*, 2004). When plastids isolated from developing sunflower embryos were supplied with a range of precursors, malate was found to support the highest rates of fatty acid synthesis throughout the period of oil accumulation. These results led to the conclusion that reducing power is largely generated via plastidic NADP-dependent malic enzyme and pyruvate dehydrogenase (Pleite *et al.*, 2005). In contrast to these findings with isolated plastids, we found that, in the intact embryo, malate provides <9% of the carbon for fatty acid synthesis, the remainder being supplied by triose-P derived from hexoses. Furthermore, our analysis revealed that the pentose-P pathway is the main provider of NADPH in developing sunflower embryos, whereas plastidic malic enzyme produces <4% of the total NADPH. Comparison of these studies suggests that isolated plastids do not quantitatively reflect fluxes that occur *in vivo*. Similar conclusions have been drawn based on comparison of fatty acid synthesis by isolated chloroplasts with *in vivo* labeling of leaves (Bao *et al.*, 2000).

Biological validation

All the experiments presented in this study were conducted under normoxic conditions. However, by measuring the activity of oleate desaturase (FAD2, EC 1.3.1.35) under different O_2 concentrations, Garcia-Diaz *et al.* (2002) suggest that storage oil synthesis of developing sunflower embryos may be O_2-limited under normal growing conditions. A recent study comparing transcript profiles in leaves and immature sunflower embryos using cDNA microarrays reported genes related to amino acid metabolism and fatty acid metabolism to be upregulated in immature embryos as well as genes of the glycolytic pathway such as fructose-bisphosphate aldolase, cytosolic glyceraldehyde-3-P dehydrogenase and pyruvate kinase (Hewezi *et al.*, 2006). The authors also reported preferential expression patterns in immature embryos for enzymes associated with the TCA cycle (NAD-dependent malate dehydrogenase, mitochondrial pyruvate dehydrogenase and isocitrate dehydrogenase), which is in agreement with the high respiratory activity that we deduced, and argues against the idea that these embryos normally grow under hypoxic conditions. No upregulation of plastidic NADP-dependent malic enzyme was found. These data are consistent with our conclusion that sunflower embryos direct substantial fluxes through the TCA cycle, and that pyruvate may be mainly produced from hexose via the glycolytic pathway and not via plastidic NADP-dependent malic enzyme.

Potential limitations of this study

Analyses of multiple metabolic fluxes depend on using models of the metabolic network to interpret labeling data, and the validity of the flux maps derived depends on these models being realistic. The risk that models may be flawed is increased when, as is the case for sunflower embryos, fewer *in vitro* enzyme activity studies or gene expression data exist than for members of the *Brassica* family. Therefore, we tested a number of other models with different or additional network connections, which included: (i) an oxidative part of the OPPP in the cytosol, (ii) a full OPPP in the cytosol, and (iii) direct entry of pyruvate from the cytosol to the plastid for oil synthesis. None of these explained the data better than the one presented here (as determined by the sum of squared weighted deviations of simulated from measured data, results not shown). To provide further confidence in the results, we used a larger number of different labeling experiments and biological replicates than in previous metabolic flux analyses of plant systems. We also tested the results of the flux mapping against independent measurements. These checks and tests persuade us that the flux map is substantially correct.

Labeling experiments in metabolic flux analysis studies are almost never carried out on intact plants in order to ensure metabolic and isotopic steady state. Potential effects of culture conditions on embryos developing in culture must therefore be considered, as the findings of metabolic flux analyses might not represent the fluxes *in planta*. In sunflower, the concentrations of substrates to which the embryo is exposed *in planta* are uncertain, although we did determine the predominant metabolites in the vascular tissue and used those substrates in culture. It is nevertheless possible that the levels of the substrates used affected the metabolic fluxes. We believe that this is unlikely because storage compound production and growth directly consume intermediates throughout central metabolism, and we verified that embryos developing in culture grew at the same rate, and produced the same storage compounds in similar proportions, as *in planta*. The NMR and MS techniques used to measure labeling in extracted metabolites and biomass compounds that are accumulating do not allow the labeling in intermediary metabolites present at low levels to be measured directly – rather they are inferred from their metabolic products (Ratcliffe and Shachar-Hill, 2006). This well-established practice might lead to erroneous conclusions about metabolic fluxes if metabolite channeling (Giege *et al.*, 2003) plays a significant role, as the labeling of one or more intermediates could be different from that inferred from product labeling in this case.

Experimental procedures

Labeled isotopes

[U-$^{14}C_6$]glucose (317 mCi mmol^{-1}, 11.7 GBq mmol^{-1}), [U-$^{14}C_5$]glutamine (242 mCi mmol^{-1}, 8.95 GBq mmol^{-1}) and [U-$^{14}C_4$]malate (52 mCi mmol^{-1}, 1.92 GBq mmol^{-1}) were obtained from Amersham Biosciences (http://www5.amershambiosciences.com/). [1-$^{13}C_1$]glucose and [U-$^{13}C_5$]glutamine were obtained from Isotec (http://www.sigmaaldrich.com). [2-$^{13}C_1$]glucose was obtained from Cambridge Isotope Laboratories Inc (http://www.isotope.com).

Plant material

Helianthus annuus L. (sunflower accession Ames 7576) was grown in 30 cm pots in a greenhouse maintained at 25°C/20°C day/night temperature with supplemental lighting to provide irradiance of approximately 600 μE m^{-2} sec^{-1} under a 16 h/8 h day/night photoperiod. At 2 weeks, seedlings were thinned to two per pot. Flowers were tagged at anthesis. Tagged seeds were harvested at 12 days after polination and taken to a laminar flow bench for dissection.

Medium composition and embryo culture conditions

Seeds were surface-sterilized with 5% sodium hypochlorite for 10 min and then rinsed three times with sterile water. The

developing embryos were dissected under aseptic conditions and transferred into culture medium comprising glucose (400 mM) and glutamine (70 mM) as carbon and nitrogen sources, respectively (malate was added at 3 mM in some experiments), minerals in the form of 4.3 g l^{-1} MS basal salts, vitamins in the form of nicotinic acid (5 μg ml^{-1}), pyridoxin hydrochloride (0.5 μg ml^{-1}), thiamine hydrochloride (0.5 μg ml^{-1}) and folic acid (0.5 μg ml^{-1}), respectively, with 10 mM MES included as a buffer, and adjusted to pH 5.8 with 1 *N* KOH. The embryos were placed on double glassfiber prefilters soaked with 10 ml of the medium previously described, and cultured for 5 days at 25°C in the dark in a 250 ml screw-cap Erlenmeyer flask sealed with a septum closure.

Determination of O_2 consumption, CO_2 efflux and $^{14}CO_2$

Immediately after culture, the flasks were placed in an ice bath and 1 ml of 0.2 *N* HCl was injected through the septum to stop metabolism and to release inorganic carbon to the flask headspace. Duplicate 200 μl gas samples were withdrawn from the flask headspace using a 1 ml syringe, and injected into an infra-red gas analyzer to determine total CO_2 efflux and O_2 consumption. As described by Goffman *et al.* (2005), the CO_2 was trapped and $^{14}CO_2$ present in the trapping solution was counted. The embryos were removed and rinsed three times each with 10 ml water to remove surface radioisotope. The embryos were then frozen with liquid nitrogen and lyophilized.

Separation of biomass compounds

Compounds (oil, proteins and cell wall) were extracted as described by Goffman *et al.* (2005) with the following modifications. To extract the oil, embryos were homogenized in an Eppendorf tube containing a tungsten bead (6 mm diameter) and 1 ml hexane:isopropanol (2:1 v/v) with a paint shaker at 4°C, and the extraction of soluble components was performed as described by Salon *et al.* (1988). For NMR analyses, the extracted metabolites were separated as neutral, acidic and cationic fractions containing the sugar, organic acid and amino acid fractions, respectively, as described by Dieuaide-Noubhani *et al.* (1995). Starch was extracted from the residue of protein extraction as described by Moing *et al.* (1994).

Determination of biomass content

Oil content was determined by gas chromatography (GC) with flame ionization detection of fatty acid methyl esters (FAMEs) as described by Goffman *et al.* (2005). Protein content was quantified using the Bradford assay (Bradford, 1976). Starch was determined using a Megazyme (http://www.megazyme.com) total starch assay kit. Cell-wall content was estimated by measuring the dry weight of the samples after all extractions.

Calculation of carbon-uptake, balance and carbon conversion efficiency

Glutamine and glucose uptake were estimated from labeling experiments in which [U-$^{14}C_5$]glutamine + unlabeled glucose or [U-$^{14}C_5$]glutamine + [U-$^{14}C_6$]glucose were supplied, by dividing the total ^{14}C incorporated by developing sunflower embryos (^{14}C in storage biomass and water-soluble molecules and $^{14}CO_2$ released) by the specific radioactivity of the substrates added to the medium. Glucose uptake was determined from the difference between the uptake of radiolabel when [U-$^{14}C_5$]glutamine + [U-$^{14}C_6$]glucose were supplied compared with that when [U-$^{14}C_5$]glutamine + unlabeled glucose were supplied. Carbon balance and carbon conversion efficiency were calculated according to the method described by Goffman *et al.* (2005) by providing all carbon sources uniformly ^{14}C-labeled at the same specific activity and determining ^{14}C incorporate into biomass end products and released as $^{14}CO_2$.

NMR analyses

^{1}H-NMR of the vascular and embryonic tissues. *Capitulum* vascular tissue and embryonic tissues were collected at 12 DAP, and the fresh weight was measured before freezing in liquid nitrogen. After lyophilization weight was measured in order to estimate the quantity of water in vascular and embryonic tissues. The extraction of soluble components was performed as described by Salon *et al.* (1988) using samples to which gallic acid had previously been added as an internal standard. The extract was dried and resuspended in 600 μl D_2O for ^{1}H-NMR analyses. ^{1}H spectra were acquired at 499.74 MHz using a Varian 500 MHz spectrophotometer (http://www.varianinc.com) at 25°C using a 5 mm probe with a 10.13 μsec pulse corresponding to a 90° angle and a relaxation time of 20 sec. The concentration of metabolites detected was calculated according to the internal standard and the quantity of water present in the tissue. Vascular exudates had similar metabolite contents to vascular tissue.

NMR analyses of labeled samples. Spectra were obtained at 25°C using a Varian 500 MHz spectrometer equipped with a 5 mm probe. The oil extract was resuspended in 600 μl deuterochloroform ($CDCl_3$), and amino acid, organic acid, sugar and starch fractions were resuspended in deuterium oxide (D_2O). ^{1}H NMR spectra were obtained at 499.74 MHz with a pulse of 10.13 μsec (corresponding to an angle of 90°) using a recycling time >6 T_1. ^{13}C NMR spectra were obtained at 125.66 MHz with a pulse of 7.08 μsec (corresponding to an angle of 90°) using a recycling time greater than 6 T_1. The absolute ^{13}C enrichments were determined as described by Rontein *et al.* (2002).

GC-MS analyses of protein hydrolysates

Proteins were hydrolyzed in 6 N HCl and the amino acids were derivatized to *N,O-tert*-butyldimethylsilyl (TBDMS) derivatives as described previously (Schwender *et al.*, 2003). TBDMS amino acids were analyzed by GC-MS. The systems comprised Agilent Technologies 5973 *N* inert mass selective detector instruments (http://www.agilent.com), an Agilent Technologies G2578A system with a 30 × 0.25 mm HP5 column (Hewlett Packard, provided by Agilent Technologies) and an Agilent Technologies G2589A system with a 60 × 0.25 mm DB5MS column (J&W Scientific; (http://www.jandw.com). The carrier gas was helium at a flow rate of 1 ml min^{-1}. The relative abundances of mass isotopomers in selected fragments of each analyzed derivative were measured using selected ion monitoring (Schwender *et al.*, 2003). Correction for the occurrence of ^{13}C in derivative parts of the molecules and for heavy isotopes in heteroatoms (C, H, O, N, Si) at their natural abundances was performed as described previously (Schwender *et al.*, 2003).

Modeling metabolic pathways

The metabolic model (Figure 5) was programmed in the 13C-FLUX format (Wiechert *et al.*, 2001) (Table S1). In order to include data

from the three separate experiments with [1-$^{13}C_1$]glucose, [2-$^{13}C_1$]glucose and [U-$^{13}C_5$]glutamine into a single flux estimation procedure, each flux and metabolite pool was programmed three times (using subscript 2 for the [2-$^{13}C_1$]glucose experiment, and U for the [U-$^{13}C_5$]glutamine experiment). Equality of identical fluxes in the separate metabolic networks thus defined was forced by using equality equations. The following net fluxes Vg, Vres, Vfas2, Vsuc1, Vglc, Valdp, Vfas1, Vppp1, Vme, Vpepc, Vwall and Vsta were set as free, whereas fluxes through amino acid synthesis were constrained to their experimental values. The exchange fluxes Vgf, Vald, Vglyco, Vgl, Vakg, Vhcp, Vppp2, Vppp3, Vppp4, Vfum1 and Vpepc were set as free, whereas Vhk, Vres, Vpk, Vpyr, Vstsp, Valpd, Vpkp, Vpdhp, Vmep, Vppp, Vpdh, Vcs, Vca, Vsfa, Vpepc and the fluxes of amino acid synthesis were constrained to 0 (irreversible). Flux values quantified by biomass composition and quantification (Vfas2, Vsuc1, Vglc, Vfas1, Vwall and Vsta), as well as Vres calculated according to the method described by Alonso *et al.* (2005), were included as measurements in the 13C-FLUX model and set as free parameters. The optimization program used was Donlp2, with over 2000 different starting points. The best fit, which was also the most commonly optimized values (69% of the fits) for the fluxes, is presented in Figure 5 and Table 1.

Acknowledgements

We are grateful to Professor Randy Beaudry for helpful advice and access to equipment for the determination of gas compositions. We thank Beverly Chamberlin of the Michigan State University GC-MS facility, Daniel Holmes of the Michigan State University NMR facility, Hart Poskar for his useful programs, and Doug Allen for helpful discussions. We acknowledge Dr Robert Stebbins from the USDA-ARS, North Central Regional Plant Introduction Station, Iowa State University, Ames, Iowa, for kindly providing the sunflower seed. This work was supported in part by USDA-NRI grant number 2006-35318-16661 to Y.S.-H. and J.B.O.

Supplementary material

The following supplementary material is available for this article online:

Figure S1. ^{1}H-NMR spectrum of the ethanolic extraction of sunflower vascular tissue.

Table S1. Metabolic network.

Table S2. Steady-state ^{13}C enrichments of metabolites after incubating sunflower embryos with [2-$^{13}C_1$]glucose, [1-$^{13}C_1$]glucose or [U-$^{13}C_5$]glutamine.

Table S3. Steady-state ^{13}C isotopomer abundance of amino acids from protein hydrolysis.

This material is available as part of the online article from http://www.blackwell-synergy.com

References

Alonso, A.P., Vigeolas, H., Raymond, P., Rolin, D. and Dieuaide-Noubhani, M. (2005) A new substrate cycle in plants. evidence for a high glucose-phosphate-to-glucose turnover from *in vivo* steady-state and pulse-labeling experiments with [C-13] glucose and [C-14] glucose. *Plant Physiol.* **138**, 2220–2232.

Bao, X., Focke, M., Pollard, M. and Ohlrogge, J. (2000) Understanding *in vivo* carbon precursor supply for fatty acid synthesis in leaf tissue. *Plant J.* **22**, 39–50.

Ben, C., Hewezi, T., Jardinaud, M., Bena, F., Ladouce, N., Moretti, S., Tamborindeguy, C., Liboz, T., Petitprez, M. and Gentzbittel, L. (2005) Comparative analysis of early embryonic sunflower cDNA libraries. *Plant Mol. Biol.* **57**, 255–270.

Bradford, M.M. (1976) Rapid and sensitive method for quantitation of microgram quantities of protein utilizing principle of protein–dye binding. *Anal. Biochem.* **72**, 248–254.

Browse, J. and Slack, C.R. (1985) Fatty-acid synthesis in plastids from maturing safflower and linseed cotyledons. *Planta*, **166**, 74–80.

Converti, A. and Perego, P. (2002) Use of carbon and energy balances in the study of the anaerobic metabolism of *Enterobacter aerogenes* at variable starting glucose concentrations. *Appl. Microbiol. Biotechnol.* **59**, 303–309.

Dieuaide-Noubhani, M., Raffard, G., Canioni, P., Pradet, A. and Raymond, P. (1995) Quantification of compartmented metabolic fluxes in maize root tips using isotope distribution from 13C- or 14C-labeled glucose. *J. Biol. Chem.* **270**, 13147–13159.

Eastmond, P.J. and Rawsthorne, S. (2000) Coordinate changes in carbon partitioning and plastidial metabolism during the development of oilseed rape embryo. *Plant Physiol.* **122**, 767–774.

Flinn, A.M., Atkins, C.A. and Pate, J.S. (1977) Significance of photosynthetic and respiratory exchanges in carbon economy of developing pea fruit. *Plant Physiol.* **60**, 412–418.

Garcia-Diaz, M.T., Martinez-Rivas, J.M. and Mancha, M. (2002) Temperature and oxygen regulation of oleate desaturation in developing sunflower (*Helianthus annuus*) seeds. *Physiol. Plant.* **114**, 13–20.

Giege, P., Heazlewood, J.L., Roessner-Tunali, U., Millar, A.H., Fernie, A.R., Leaver, C.J. and Sweetlove, L.J. (2003) Enzymes of glycolysis are functionally associated with the mitochondrion in Arabidopsis cells. *Plant Cell*, **15**, 2140–2151.

Goffman, F.D., Alonso, A.P., Schwender, J., Shachar-Hill, Y. and Ohlrogge, J.B. (2005) Light enables a very high efficiency of carbon storage in developing embryos of rapeseed. *Plant Physiol.* **138**, 2269–2279.

Hargreaves, J.A. and ap Rees, T. (1988) Turnover of starch and sucrose in roots of *Pisum sativum*. *Phytochemistry*, **27**, 1627–1629.

Hatzfeld, W.D. and Stitt, M. (1990) A study of the rate of recycling of triose phosphates in heterotrophic *Chenopodium rubrum* cells, potato-tubers, and maize endosperm. *Planta*, **180**, 198–204.

Hewezi, T., Petitprez, M. and Gentzbittel, L. (2006) Primary metabolic pathways and signal transduction in sunflower (*Helianthus annuus* L.): comparison of transcriptional profiling in leaves and immature embryos using cDNA microarrays. *Planta*, **223**, 948–964.

Hill, S.A. and ap Rees, T. (1994) Fluxes of carbohydrate-metabolism in ripening bananas. *Planta*, **192**, 52–60.

Hill, S.A. and ap Rees, T. (1995) The effect of hypoxia on the control of carbohydrate-metabolism in ripening bananas. *Planta*, **197**, 313–323.

Hill, L.M. and Smith, A.M. (1991) Evidence that glucose-6-phosphate is imported as the substrate for starch synthesis by the plastids of developing pea embryos. *Planta*, **185**, 91–96.

Hsu, F.C. and Obendorf, R.L. (1982) Compositional analysis of in vitro matured soybean seeds. *Plant Sci. Lett.* **27**, 129–135.

Kang, F. and Rawsthorne, S. (1996) Metabolism of glucose-6-phosphate and utilization of multiple metabolites for fatty acid synthesis by plastids from developing oilseed rape embryos. *Planta*, **199**, 321–327.

Kang, F., Ridout, C.J., Morgan, C.L. and Rawsthorne, S. (1994) The activity of acetyl-CoA carboxylase is not correlated with the rate of lipid-synthesis during development of oilseed rape (*Brassica napus* L) embryos. *Planta*, **193**, 320–325.

Kleppinger-Sparace, K.F., Stahl, R.J. and Sparace, S.A. (1992) Energy-requirements for fatty-acid and glycerolipid biosynthesis from acetate by isolated pea root plastids. *Plant Physiol.* **98**, 723–727.

Mantese, A.I., Medan, D. and Hall, A.J. (2006) Achene structure, development and lipid accumulation in sunflower cultivars differing in oil content at maturity. *Ann. Bot.* **97**, 999–1010.

Moing, A., Escobar-Gutierrez, A. and Gaudillere, J.P. (1994) Modeling carbon export out of mature peach leaves. *Plant Physiol.* **106**, 591–600.

Mollney, M., Wiechert, W., Kownatzki, D. and de Graaf, A.A. (1999) Bidirectional reaction steps in metabolic networks: IV. Optimal design of isotopomer labeling experiments. *Biotechnol. Bioeng.* **66**, 86–103.

Neuhaus, H.E., Batz, O., Thom, E. and Scheibe, R. (1993) Purification of highly intact plastids from various heterotrophic plant-tissues – analysis of enzymatic equipment and precursor dependency for starch biosynthesis. *Biochem. J.* **296**, 395–401.

Novak, L. and Loubiere, P. (2000) The metabolic network of *Lactococcus lactis*: distribution of C-14-labeled substrates between catabolic and anabolic pathways. *J. Bacteriol.* **182**, 1136–1143.

Pate, J.S., Sharkey, P.J. and Atkins, C.A. (1977) Nutrition of a developing legume fruit – functional economy in terms of carbon, nitrogen, water. *Plant Physiol.* **59**, 506–510.

Peoples, M.B., Pate, J.S., Atkins, C.A. and Murray, D.R. (1985) Economy of water, carbon, and nitrogen in the developing cowpea fruit. *Plant Physiol.* **77**, 142–147.

Pleite, R., Pike, M.J., Garces, R., Martinez-Force, E. and Rawsthorne, S. (2005) The sources of carbon and reducing power for fatty acid synthesis in the heterotrophic plastids of developing sunflower (*Helianthus annuus* L.) embryos. *J. Exp. Bot.* **56**, 1297–1303.

Ploschuk, E.L. and Hall, A.J. (1997) Maintenance respiration coefficient for sunflower grains is less than that for the entire capitulum. *Field Crops Res.* **49**, 147–157.

Qi, Q.G., Kleppinger-Sparace, K.F. and Sparace, S.A. (1995) The utilization of glycolytic-intermediates as precursors for fatty-acid biosynthesis by pea root plastids. *Plant Physiol.* **107**, 413–419.

Ratcliffe, R.G. and Shachar-Hill, Y. (2005) Revealing metabolic phenotypes in plants: inputs from NMR analysis. *Biol. Rev.* **80**, 27–43.

Ratcliffe, R.G. and Shachar-Hill, Y. (2006) Measuring multiple fluxes through plant metabolic networks. *Plant J.* **45**, 490–511.

Rawsthorne, S. (2002) Carbon flux and fatty acid synthesis in plants. *Progr. Lipid Res.* **41**, 182–196.

Rontein, D., Dieuaide-Noubhani, M., Dufourc, E.J., Raymond, P. and Rolin, D. (2002) The metabolic architecture of plant cells. Stability of central metabolism and flexibility of anabolic pathways during the growth cycle of tomato cells. *J. Biol. Chem.* **277**, 43948–43960.

Roughan, P.G., Holland, R. and Slack, C.R. (1979) Control of long-chain fatty acid synthesis in isolated intact spinach (*Spinacia oleracea*) chloroplasts. *Biochem. J.* **184**, 193–202.

Ruuska, S.A., Schwender, J. and Ohlrogge, J.B. (2004) The capacity of green oilseeds to utilize photosynthesis to drive biosynthetic processes. *Plant Physiol.* **136**, 2700–2709.

Saez, J.C., Schell, D.J., Tholudur, A., Farmer, J., Hamilton, J., Colucci, J.A. and McMillan, J.D. (2002) Carbon mass balance evaluation of cellulase production on soluble and insoluble substrates. *Biotechnol. Prog.* **18**, 1400–1407.

Salon, C., Raymond, P. and Pradet, A. (1988) Quantification of carbon fluxes through the tricarboxylic-acid cycle in early germinating lettuce embryos. *J. Biol. Chem.* **263**, 12278–12287.

Schwender, J., Ohlrogge, J.B. and Shachar-Hill, Y. (2003) A flux model of glycolysis and the oxidative pentosephosphate pathway in developing *Brassica napus* embryos. *J. Biol. Chem.* **278**, 29442–29453.

Schwender, J., Goffman, F., Ohlrogge, J.B. and Shachar-Hill, Y. (2004a) Rubisco without the Calvin cycle improves the carbon efficiency of developing green seeds. *Nature*, **432**, 779–782.

Schwender, J., Ohlrogge, J. and Shachar-Hill, Y. (2004b) Understanding flux in plant metabolic networks. *Curr. Opin. Plant Biol.* **7**, 309–317.

Schwender, J., Shachar-Hill, Y. and Ohlrogge, J.B. (2006) Mitochondrial metabolism in developing embryos of *Brassica napus*. *J. Biol. Chem.* **281**, 34040–34047.

Smith, R.G., Gauthier, D.A., Dennis, D.T. and Turpin, D.H. (1992) Malate-dependent and pyruvate-dependent fatty-acid synthesis in leukoplastids from developing castor endosperm. *Plant Physiol.* **98**, 1233–1238.

Sriram, G., Fulton, D.B., Iyer, V.V., Peterson, J.M., Zhou, R.L., Westgate, M.E., Spalding, M.H. and Shanks, J.V. (2004) Quantification of compartmented metabolic fluxes in developing soybean embryos by employing biosynthetically directed fractional C-13 labeling, [C-13, H-1] two-dimensional nuclear magnetic resonance, and comprehensive isotopomer balancing. *Plant Physiol.* **136**, 3043–3057.

Weaire, P.J. and Kekwick, R.G.O. (1975) Fractionation of fatty-acid synthetase activities of avocado mesocarp plastids. *Biochem. J.* **146**, 439–445.

Wiechert, W. and de Graaf, A.A. (1997) Bidirectional reaction steps in metabolic networks. 1. Modeling and simulation of carbon isotope labeling experiments. *Biotechnol. Bioeng.* **55**, 101–117.

Wiechert, W., Siefke, C., de Graaf, A.A. and Marx, A. (1997) Bidirectional reaction steps in metabolic networks. 2. Flux estimation and statistical analysis. *Biotechnol. Bioeng.* **55**, 118–135.

Wiechert, W., Mollney, M., Isermann, N., Wurzel, W. and de Graaf, A.A. (1999) Bidirectional reaction steps in metabolic networks: III. Explicit solution and analysis of isotopomer labeling systems. *Biotechnol. Bioeng.* **66**, 69–85.

Wiechert, W., Mollney, M., Petersen, S. and de Graaf, A.A. (2001) A universal framework for C-13 metabolic flux analysis. *Metab. Eng.* **3**, 265–283.

Zaitseva, M.G., Kasumova, I.V., Kasumov, E.A., Borisova, M.A. and Il'chishina, N.V. (2002) Respiration of mitochondria in developing sunflower seeds. *Biol. Bulletin*, **29**, 555–558.

